On the real catalytically active species for CO_2 fixation into cyclic carbonates under near ambient conditions: Dissociation equilibrium of [BMIm][Fe(NO)$_2$Cl$_2$] dependant on reaction temperature

Meike K. Leu,[†] Isabel Vicente,[†] Jesum Alves Fernandes,[¥] Imanol de Pedro,[§] Jairton Dupont,[†,‡] Victor Sans,[†] Peter Licence,[†,¥] Aitor Gual*,[†,1] and Israel Cano*,[†]

[†] GSK Carbon Neutral Laboratory for Sustainable Chemistry, University of Nottingham, NG7 2GA, Nottingham, UK

[¥] School of Chemistry, University of Nottingham, NG7 2RD, Nottingham, UK

[§] CITIMAC, Facultad de Ciencias, Universidad de Cantabria, 39005 Santander.

[‡] Laboratory of Molecular Catalysis, Institute of Chemistry, UFRGS, Av. Bento Gonçalves, 9500, Porto Alegre 91501-970, RS, Brazil.

ABSTRACT: An imidazolium based iron-containing ionic liquid [BMIm][Fe(NO)$_2$Cl$_2$] (BMIm = 1-*n*-butyl-3-methyl-imidazolium) has been synthesized for the first time and fully characterized employing a wide range of techniques. The iron-based containing ionic liquid was found to be an active catalyst for the cycloaddition of CO_2 to epoxides, giving high conversions for various substrates under near ambient conditions. In addition, the catalytic system showed a good recycling performance for five consecutive reaction cycles. Key mechanistic studies demonstrated that a bifunctional catalytic system is generated *in situ* by the partial dissociation of the iron-based ionic liquid into [BMIm][Cl], which results in a very efficient catalyst without the need of any additive or co-catalyst. The metal center plays a role as Lewis acid and activate the epoxide group, and the chloride anion, as part of [BMIm][Cl] moiety, acts as nucleophile and leads to the ring opening through a nucleophilic attack on the less sterically-hindered Cβ. The process is favoured by an interaction *via* H-bonding between the substrate and the H–C2 of the imidazolium ring, as was demonstrated by additional experiments. Kinetic studies indicated that the process followed first-order kinetics with respect to epoxide concentration and proved the existence of a reversible coordination/de-coordination equilibrium in which the active species are generated from the [BMIm][Fe(NO)$_2$Cl$_2$] complex.

Keywords: Bifunctional catalyst • CO_2 cycloaddition • Iron-containing ionic liquid • Kinetic studies • Mechanistic studies

---

* Corresponding authors.

E-mail address: israel.canorico@nottingham.ac.uk (Israel Cano); aitor.gual@ctqc.org (Aitor Gual).

[1] Present address: Centre Tecnológic de la Química de Catalunya (CTQC), Carrer de Marcel·lí Domingo s/n, 43007 Tarragona, Spain.

1. Introduction

In recent years, the fixation and utilization of carbon dioxide (CO_2) has become a highly important topic.[1-13] These processes are very advantageous because CO_2 is a very abundant, non-flammable, non-toxic and cheap C1 building block for organic synthesis.[14-18] Additionally, CO_2 fixation is benign from an environmental protection standpoint.[1-13] In this context, the insertion of CO_2 into epoxides to form five-membered cyclic carbonates has attracted large interest,[19-25] since these compounds show industrial applications as polar aprotic solvents, electrolytes for batteries, starting materials for the formation of polymers and relevant intermediates in the preparation of fine chemicals and pharmaceutical compounds, amongst others.[20, 26-31] Consequently, the cycloaddition of carbon dioxide to oxiranes has been described by the use of a large range of catalytic systems, such as amines and phosphines,[32-35] frustrated Lewis pairs (FLPs),[36] alkali metals,[37] metal oxides,[38, 39] organometallic complexes,[21, 24, 40-44] metal-organic frameworks[45-47] and carbon materials.[48-51] Specifically, ionic liquids (ILs) have received much attention in this research field because they possess important properties that make them very suitable as catalysts, including good thermal stability, high catalytic activity, ease of catalyst recovery and product purification, high capability for CO_2 capture and solvation, and easy fine-tuning basicity-nucleophilicity by simple modification of the IL structure (anion and cation).[21, 52-59] Furthermore, the use of metal halides or metal complexes with Lewis acid properties as co-catalyst improves the catalytic performance of ILs.[52] In this way, metal-containing ILs have shown to exhibit a particular ability to perform this transformation. This type of systems operates as a bifunctional catalyst acting .simultaneously as Lewis acid and as nucleophile. However, the identification of the real catalyst is a difficult task since different ionic species can be generated in the reaction medium during the process.[60, 61] To the best of our knowledge, only a few examples have been reported in which well-defined metal-containing ILs were used as catalysts for the cycloaddition of CO_2 to epoxides.[62-65]

In the present work we report the use of a novel imidazolium based iron-containing ionic liquid [BMIm][Fe(NO)$_2$Cl$_2$] (BMIm = 1-*n*-butyl-3-methyl-imidazolium) as a bifunctional catalyst for the in-depth study and understanding of the formation mechanism of cyclic carbonates *via* cycloaddition of CO_2 with epoxides by metal-containing ILs. To this end, we have employed μ,μ'-dichloro-tetranitrosyl-diiron ([Fe(NO)$_2$Cl]$_2$) as metallic precursor for the formation of the Fe-based ionic liquid. This precursor was chosen because it was found to generate only well-defined monometallic species during the synthetic process. An exhaustive characterization was carried out by different techniques, which demonstrated that [BMIm][Fe(NO)$_2$Cl$_2$] is the actual structure of the Fe-containing ionic liquid. Such a complex was found to be a highly active catalyst under very mild conditions, giving high conversions and chemoselectivities for a wide range of substrates without the need of any additive. Furthermore, the catalytic system was successfully recycled and only minor deactivation was

observed after five cycles. More importantly, the role of the different species involved in the catalytic cycle of this transformation was established by experimental kinetic and mechanistic studies.

2. Experimental

2.1. General Procedures

All oxygen and moisture sensitive operations were carried out under an argon atmosphere using standard vacuum-line and Schlenk techniques. Solvents were purchased from Sigma-Aldrich as HPLC grade and dried by means of an Inert Puresolv MD purification system. All reagents were purchased from Sigma Aldrich and purified when required by literature procedures.[66] Elemental analyses (EA) were performed by the Elemental Analysis Service of the University of Nottingham.

2.2. Instrumentation

2.2.1. Thermogravimetric Analysis (TGA)

Thermogravimetric measurements were carried out on a TA instruments Discovery at a heating rate of 10 °C/min and in a temperature range from 20 to 1000 °C under N_2 in a platinum crucible.

2.2.2. Inductively Coupled Plasma Optical Emission Spectrometry (ICP-OES)

The iron and chloride content determination was performed through analysis of the samples by ICP-OES on a Perkin Elmer Optima 2000 DV ICP-OES. The samples were prepared by diluting 25 mL of ionic liquid with approximated iron concentration of 150 mg/L (ppm) (and, when chloride is present, the chloride concentration is between 100-150 mg/L (ppm) in HNO_3 with a concentration of 2 % (v/V). Calibration curves were prepared using standard solutions of concentrations between 0 to 250 ppm for iron and 0 to 800 ppm for chloride prepared by dilution of the standard solution. The iron and chloride Standard for ICP TraceCERT® (10′000 mg/L Fe in nitric acid and 10'000 mg/L Cl in water) were supplied by Sigma Aldrich.

2.2.3. Electrospray Ionization Mass spectrometry (ESI-MS)

ESI-MS analyses were carried out on a Bruker ESI-TOF MicroTOF II.

2.2.4. Fourier Transform Infrared Spectroscopy (ATR FT-IR)

ATR FT-IR measurements were performed on a Bruker Alpha Series FT-IR spectrometer equipped with an attenuated total reflectance (ATR) module. The ATR FT-IR spectra were recorded by collecting 16 scans of a compound in the ATR module.

2.2.5. Raman Spectroscopy

Raman spectroscopy was carried out on a Horiba LabRAM HR at room temperature.

2.2.6. Electron Paramagnetic Resonance (EPR)

EPR analyses were performed on a Bruker EMX with Bruker ER041XG Microwave bridge (X-band) at room temperature (R.T.) and at 77 K in a quartz dewar.

2.2.7. X-ray Photoelectron Spectroscopy (XPS)

XPS measurements were carried out using a Kratos AXIS Ultra DLD instrument. The chamber pressure during the measurements was 5×10^{-9} Torr. Wide energy range survey scans were collected

at a pass energy of 80 eV in hybrid slot lens mode and a step size of 0.5 eV. High-resolution data on the C 1s, Cl 2p, N 1s and Fe 2p photoelectron peaks was collected at pass energy 20 eV over energy ranges suitable for each peak, and collection times of 5 min, step sizes of 0.1 eV. The charge neutraliser filament was used to prevent the sample charging over the irradiated area. The X-ray source was a monochromated Al Kα emission, run at 10 mA and 12 kV (120 W). The energy range for each 'pass energy' (resolution) was calibrated using the Kratos Cu $2p_{3/2}$, Ag $3d_{5/2}$ and Au $4f_{7/2}$ three-point calibration method. The transmission function was calibrated using a clean gold sample method for all lens modes and the Kratos transmission generator software within Vision II. The data were processed with CASAXPS (Version 2.3.17). Peaks were fitted using GL(30) line shapes (70% Gaussian and 30% Lorentzian). The wide scan and high resolution spectra were calibrated to the alkyl chain at 285.0 eV.[67]

2.2.8. Magnetization measurements

DC magnetic susceptibility measurement was performed using Quantum Design PPMS magnetometer whilst heating from 2 to 300 K under an applied magnetic field of strength 1 kOe. Magnetization as a function of field (H) was measured using the same magnetometer in the $-80 \leq H/kOe \leq 80$ at 2 K after cooling the sample in zero field.

2.3. Synthesis of iron-containing ionic liquids

1-Butyl-3-methylimidazolium chloride[68] ([BMIm]Cl), 1-butyl-2,3-dimethylimidazolium chloride[68] ([BMMIm]Cl) and μ-dichloro-tetranitrosyl-diiron[69] ([Fe(NO)$_2$Cl]$_2$) were synthesized according to standard procedures described in the literature. The chosen amount of [Fe(NO)$_2$Cl]$_2$ was mixed with 2 equivalents of salt ([BMIm]Cl, [BMMIm]Cl or tetrabutylammonium chloride) in a Schlenk flask under Ar atmosphere. After stirring for 12 h at room temperature (R.T.), a black liquid was obtained. The so-obtained metal-containing ionic liquids were characterized by ICP-OES, EA, ESI-MS, FT-IR and EPR. In addition, the iron-containing ionic liquid [BMIm][Fe(NO)$_2$Cl$_2$ was also characterized by TGA, XPS, Raman and magnetic susceptibility measurements. Full characterization data, spectra and specific synthetic procedures are available in the supporting information.

2.4. Catalytic experiments

2.4.1. Formation of carbonates

Catalytic experiments were carried out in a small reactor with a total volume of 2 mL. In a standard reaction, the chosen amount of Fe-based ionic liquid was mixed with the required quantity of epoxide in a glass vial with a magnetic stirrer. The reactor was flushed with carbon dioxide (CO_2) three times before the pressure was kept constant at the desired pressure using a reservoir and was heated at the desired temperature. After the specified time, the reactor was cooled to R.T. and slowly depressurized. The product was purified by extraction with diethyl ether (2 x 5 mL) and filtration with SiO_2 by flash chromatography. Afterwards, the solvent was evaporated to dryness at 150 mbar and R.T. using a rotary evaporator. The residue was dissolved in CDCl$_3$ and analyzed by ^{1}H NMR to determine conversion and selectivity.

2.4.2. Formation of diols

Catalytic experiments were carried out in a small Schlenk flask. In a standard reaction, 10 mol% of the Fe-based ionic liquid **1** was mixed with 200 mg of styrene oxide and 1 mL of H_2O in a Schlenk flask under Ar atmosphere with a magnetic stirrer. After 24 h, the product was purified by extraction with diethyl ether (2 x 5 mL) and filtration with SiO_2 by flash chromatography. Afterwards, the solvent was evaporated to dryness at 150 mbar and R.T. using a rotary evaporator. The residue was dissolved in $CDCl_3$ and analyzed by ^{1}H NMR to determine conversion and selectivity.

2.4.3. Recycling experiments

Recycling experiments were carried out in a Fisher-Porter reactor. In a standard reaction, 5 mol% of the Fe-based ionic liquid **1** was mixed with the chosen amount of epoxide (200 mg for styrene oxide, 283 mg for 1,2-epoxypentane) and equipped with a magnetic stirrer. The reactor was flushed with CO_2 three times before the pressure was kept constant at 2 bar using a reservoir and was heated at the desired temperature (40 °C for styrene oxide, 80 °C for 1,2-epoxypentane). After 24 h, the reactor was cooled to R.T. and slowly depressurized. The product was purified by extraction with diethyl ether (2 x 5 mL) and centrifugation to recover the catalyst. Afterwards, the solvent was evaporated to dryness at 150 mbar and R.T. using a rotary evaporator. The residue was dissolved in $CDCl_3$ and analyzed by ^{1}H NMR to determine conversion and selectivity. **1** was recovered through re-precipitation of the insoluble fraction, which was left after the extraction of the product with diethyl ether. The catalyst was then used for the next cycle. The study of the mass balance through ^{1}H NMR spectroscopy by the use of mesitylene as internal standard enabled to confirm that substrates and products were completely extracted.

2.4.4. Kinetic studies

Experiments were carried out in a Fisher-Porter reactor with the possibility to take samples during the reaction without depressurizing the reactor. In a standard reaction, 10 mL of styrene oxide, and the chosen amount of Fe-based ionic liquid **1** were charged into the reactor equipped with a magnetic stirrer. The reactor was flushed with CO_2 three times before the pressure was kept constant at the desired pressure using a reservoir and was heated at the desired temperature. In the first hour of the reaction, samples were taken every 15 minutes and afterwards every hour. After the specified time, the reactor was cooled to R.T. and slowly depressurized. The product was purified by extraction with diethyl ether and filtration with SiO_2 by flash chromatography. Afterwards, the solvent was evaporated to dryness at 150 mbar and R.T. using a rotary evaporator. The residue was dissolved in $CDCl_3$ and analyzed by ^{1}H NMR to determine conversion and selectivity.

### 2.4.5. Radical scavenger experiments

Radical scavenger experiments were carried out in a small reactor with a total volume of 2 mL. In a standard reaction, 5 mol% of the Fe-based ionic liquid catalyst **1** was mixed with 400 mg of epoxide, and 2.5 mol% of a radical scavenger (galvinoxyl or 2,2-diphenyl-1-picrylhydrazyl (DPPH)) and equipped with a magnetic stirrer. The reactor was flushed with CO_2 three times before the pressure

was kept constant at 2 bar using a reservoir and was heated to 40 °C. After 48 h, the reactor was cooled to R.T. and slowly depressurized. The product was purified by extraction with diethyl ether and filtration with SiO_2 by flash chromatography. Afterwards, the solvent was evaporated to dryness at 150 mbar and R.T. using a rotary evaporator. The residue was dissolved in $CDCl_3$ and analyzed by ^1H NMR to determine conversion and selectivity.

3. Results and discussion

3.1. Characterization of Iron-Containing Ionic Liquid [BMIm][Fe(NO)₂Cl₂]

The treatment of μ,μ'-dichloro-tetranitrosyl-diiron ($[Fe(NO)_2Cl]_2$) with 2 equivalents of 1-butyl-3-methylimidazolium chloride ([BMIm]Cl) at R.T. affords the new Fe-based ionic liquid [BMIm][Fe(NO)₂Cl₂] (**1**) (Scheme 1).
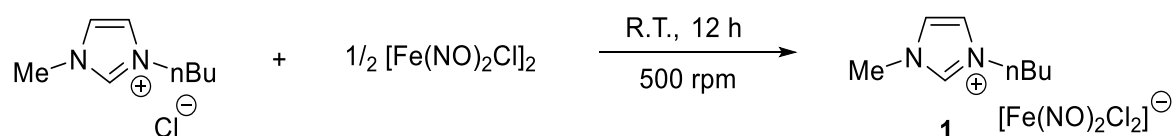
Scheme 1. Formation of [BMIm][Fe(NO)₂Cl₂] (**1**).

Due to the paramagnetic nature of the sample, NMR is not an appropriate spectroscopic tool to analyze the Fe-containing ionic liquid. The complex [BMIm][Fe(NO)₂Cl₂] was fully characterized by the use of a wide range of techniques, including TGA, EA, ICP-OES, ESI-MS, EPR, XPS, magnetic susceptibility measurements, and ATR FT-IR and Raman spectroscopies.

ICP gave an Fe content of *ca.* 16.9%, which is in good agreement with the expected value (17.1%), whereas TGA showed that the reproducibility is high (*ca.* 18.6%, see Figure S1, Supporting Information). It is worth noting that ESI-MS spectrum in the positive mode exhibits a very intense mass peak corresponding to the imidazolium cation, suggesting that it remains intact in the complex **1** (for further details see Section 2, Supporting Information). Interestingly, a low intensity peak with m/z = 464.1152 attributable to a species with two imidazolium cations and one N-bound dinitrosyl iron complex $\{[Fe(NO)_2Cl_2]^-\}$ (DNIC, $\{Fe-(NO)_2\}^9$ in the Enemark-Feltham notation) unit ($\{[BMIm]_2[Fe(NO)_2Cl_2]\}^+$) was also identified (Figure S2, Supporting Information).[70]

Metal complexes with nitrosyl ligands bound to the metal center can exist in a bent (M–N–O angle 120-140°) or linear (M–N–O angle 160-180°) mode or as an equilibrium between the two forms. Nevertheless, it was found that the two forms have different charges and electron donation. In general, the bent NO ligand is considered as [NO⁻] and the linear NO ligand as [NO⁺].[71] Therefore, the oxidation state of the metal changes depending on the type of nitrosyl ligand. Consequently, a series of spectroscopic and magnetic studies were carried out in order to elucidate the nature of the NO ligand and the oxidation state of the iron center. The $[Fe(NO)_2(\mu\text{-}Cl)]_2$ precursor is diamagnetic and thus does not give any signal in the X-band EPR spectrum.[69] Conversely, the X-band EPR spectrum

of **1** (Figure 1) indicates the presence of one main iron-nitrosyl species in solution. The signal at g value 2.01 could be assigned to the iron-nitrosyl complex. Generally, the EPR spectra of N-bound mononitrosyl iron (MNIC) $\{Fe-NO\}^7$ and N-bound dinitrosyl iron (DNIC) $\{Fe-(NO)_2\}^9$ complexes typically show g values comparable to those described herein.[72-74] Indeed, DNIC $\{Fe-(NO)_2\}^9$ present in $(Et_4N)[FeCl_2(NO)_2]$ displayed very similar EPR X-band signals ($g_{iso} = 2.03$) at 293 K in 2-MeTHF.[73, 74] However, the presence of MNIC $\{Fe-NO\}^7$ was not completely discarded because the signals reported herein are also related to MNIC $\{Fe-NO\}^7$ complexes dissolved in imidazolium ILs (i.e., 1-ethyl-3-methyl-imidazolium triflate ([EMIm][OTf]) and dicyanamide ([EMIm][dca]) ILs) and solutions of [Fe(edta)(NO)],[75, 76] [(1,4,7-trimethyl-1,4,7-triazacyclononane)-Fe(NO)(N$_3$)$_2$][77] and $[Fe(H_2O)_5NO]Cl_2$.[78]

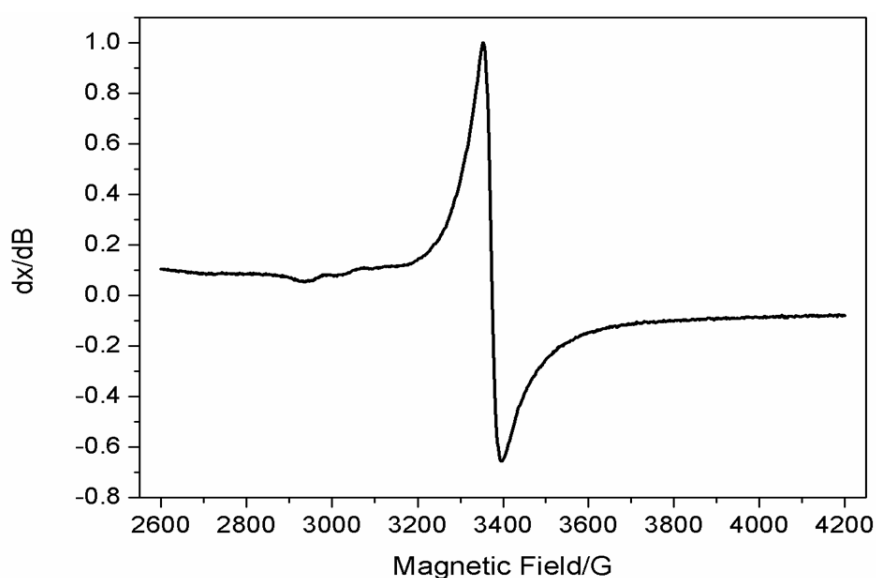**Figure 1.** EPR spectrum of **1** at R.T. in 2-methyltetrahydrofuran.

The FT-IR spectrum of the complex precursor $[Fe(NO)_2(\mu-Cl)]_2$ showed two intense bands at 1722 and 1822 cm^{-1} belonging to the NO stretching absorption (Figure S3, Supporting Information).[69] Such stretching bands were visible, although slightly shifted (1700 and 1779 cm^{-1}), in the FT-IR spectrum of **1** (Figure S3, Supporting Information), indicating the presence of NO fragments in the Fe-containing ionic liquid. These IR frequencies are comparable to those reported for $(Et_4N)[FeCl_2(NO)_2]$ (1765 and 1692 cm^{-1}), thus suggesting that similar DNIC $\{[Fe(NO)_2Cl_2]^-\}$ species are present in both complexes.[73, 74]

In addition, the IR data reported in the literature for other iron-nitrosyl complexes[79] support the presence of an iron species formally written as $\{Fe^{III}-(NO^-)_2\}$. For high-spin iron-nitrosyl complexes, the strength of the Fe−NO and N−O bonds is strongly influenced by the effective nuclear charge on iron.[72] In these $\{Fe^{III}-(NO^-)_2\}$ systems, the nitrosyl unit behaves as a relatively weak π-acceptor rather than a strong π-donor. In a complex with an anionic set of ligands, the effective nuclear charge

on iron is decreased, reducing the π-donation from the NO$^-$ orbitals. This leads to weaker N–O and Fe–NO bonds, and thus lowers the NO stretching frequency. In general, linear M–N–O groups absorb in the range 1650–1900 cm^{-1}, whereas bent M–N–O species absorb in the range 1525–1690 cm^{-1}. Then, the variations in vibrational frequencies reflect the different N–O bond orders for linear (triple bond) and bent (double bond) NO species. The displacement of anionic ligands by neutral ones rises the effective charge on iron, which is compensated by an increased donation from the [NO$^-$] ligand. For instance, NO stretching frequencies of 1810 cm^{-1} in water and 1767 cm^{-1} in [EMIm][OTf]/[EMIm][Cl] mixtures have been described for MNIC $\{Fe{-}NO\}^7$ coordinated only to neutral (H$_2$O, i.e., [Fe(H$_2$O)$_5$NO]Cl$_2$) or anionic (Cl$^-$, .i.e., [EMIm][FeCl$_3$NO]) ligands, respectively.[79] In the present case, the observed frequencies (1700 and 1779 cm^{-1}) resembled more to nitrosyl groups of iron centers mostly coordinated by anionic ligands (Cl$^-$) such as that observed for MNIC $\{Fe^{II}{-}NO^{\cdot}\}^7$ and DNIC $\{Fe^{III}{-}(NO^-)_2\}^9$ complexes.[73, 74, 79] Nevertheless, the IR measurements suggest that the presence of MNIC $\{Fe^{II}{-}NO^{\cdot}\}^7$ together with the expected DNIC $\{Fe^{III}{-}(NO^-)_2\}^9$ compound cannot be fully discarded.

The presence of the iron-nitrosyl moiety in **1** was also confirmed by analysis of the Raman spectrum, which displayed a narrow peak at *ca*. 507 cm^{-1} identified as the Fe–NO stretch vibration (Figure S4, Supporting Information). Additionally, the Raman spectrum of **1** showed a broad signal at *ca.* 311 cm^{-1}. Such a vibration frequency is consistent with the values found in the literature for the symmetric stretching mode of the Fe–Cl bond.[80-82]

On the other hand, the molar magnetic susceptibility of the Fe-based IL (Figure S5) is in good agreement with that found in other metal ILs based on [FeCl$_4^-$] ion.[80, 83, 84] The effective magnetic moment (μ_{eff}), obtained by fitting of the inverse of molar magnetic susceptibility using the Curie–Weiss law (Figure S5, blue) has a value of 5.95 (μ_B/molecule), which agrees with the expected value of 5.92 μ_B for Fe^{3+} ion.[80] Moreover, the magnetization data (see inset in Figure S5) tends to saturate above 50 kOe with a value of 5.11 m$_B$/Fe ion at 80 kOe, which is near from the expected fully saturated value of 5 m$_B$/Fe for a Fe^{3+} ion. Both data are a fingerprint indicating that Fe^{3+} is the main oxidation state of iron in the metal-based IL.

Finally, complex **1** was investigated by XPS in order to evaluate the stoichiometry and the valence state of Fe (Section 8, Supporting Information). Figure S6 shows the high resolution spectra of C 1s, Fe 2p and Cl 2p for [BMIm][Fe(NO)$_2$Cl$_2$]. The C 1s signal was deconvoluted into four components assigned to the alky chain, *N*-bond methyl and methylene carbons, and imidazolium ring carbons (Figure S6, Supporting Information).[67] The Fe 2p$_{3/2}$ signal was deconvoluted in three broad peaks typical of paramagnetic metal species.[67] The signal at 710.2 eV is assigned to $\{Fe^{III}{-}NO^-\}$ in $\{[BMIm][Fe(NO)_2Cl_2]\}$, while the signal at 712.2 eV could be associated to small fractions of species generated by decomposition of $\{[Fe(NO)_2Cl_2]^-\}$ and with similar electronic properties to that of FeCl$_2$ (i.e., MNIC $\{Fe^{II}{-}NO^{\cdot}\}^7$ $\{[Fe^{II}(NO)Cl_2]\}$ or other DNIC $\{Fe^{III}{-}(NO^-)_2\}^9$ species $\{[Fe^{III}(NO)_2Cl]\}$; Figure S6, Supporting Information).[67, 85-87] The decomposition pathway can occur through a

similar equilibrium to that described by van Eldik *et al.*, in which the rate of decomposition of the nitrosyl product is favoured with an increase of temperature (in the range 10–35 °C).[79]

3.2. Catalytic Formation of Carbonates by Cycloaddition of CO_2 with Epoxides Catalyzed by [BMIm][Fe(NO)$_2$Cl$_2$]

We decided to evaluate the catalytic performance of the Fe-based ionic liquid [BMIm][Fe(NO)$_2$Cl$_2$] in the formation of cyclic carbonates by reaction of styrene oxide with CO_2 under mild pressure and temperature conditions (Scheme 2). Further analysis of the reaction mixture revealed the presence of two side products, 2-chloro-1-phenylethanol (**B**) and 2-chloro-2-phenylethanol (**C**), which were generated in addition to the expected carbonate (Scheme 2), suggesting some stabilization process of chlorinated intermediates.
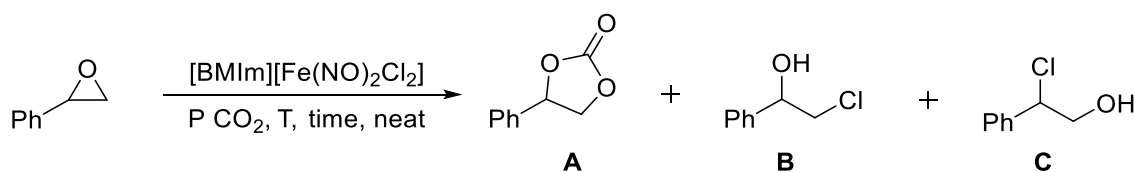
Scheme 2. Cycloaddition of CO_2 with styrene oxide catalyzed by [BMIm][Fe(NO)$_2$Cl$_2$] (**1**).

Table 1 shows the results of the catalytic optimization experiments. At R.T., 10 mol% catalyst loading and 1 bar of CO_2 pressure, low conversion was observed in 7 h (entry 1, 21%). In 24 h, 58% of conversion with chemoselectivity of 85% to the carbonate was obtained (entry 2). Increasing the temperature to 40 °C, quantitative conversion of the substrate with 87% selectivity was observed (entry 3). When the pressure was increased to 2 bar, higher conversions were observed and the selectivity to the expected product was maintained (83-84% selectivity, entries 5 and 6). The catalyst loading was found to be relatively important. While a decrease in the catalyst loading to 5 mol% at 1 bar involved a significant decrease in the conversion (entry 4, 66%), the same catalyst loading at 2 bar gave quantitative conversion with high selectivity (entry 7, 94% selectivity). However, a decrease in the catalyst loading to 2.5 mol% gave much lower conversion (entry 8, 51%). Moreover, the use of higher pressures did not improve the selectivity (entries 9 and 10). Finally, the addition of H_2O led to a decrease in the activity, which indicates some decomposition and/or deactivation process of the catalyst (entries 11 and 12). Furthermore, a decrease in the selectivity was also observed. Importantly, the catalytic system does not require the use of any solvent to perform the process.[88] Under the optimal reaction parameters based on 24 h as reaction time, 40 °C and 2 bar of CO_2 pressure, quantitative conversion and 94% chemoselectivity (entry 7) were achieved (TON = 20, TOF = 0.83 h^{-1}). It is worth noting that there are not many reported catalytic systems that proceed under mild conditions such as those described herein.[22, 24] What is more, the majority of the described systems require the use of a co-catalyst to carry out the catalytic process. On the contrary, **1** operates as a bifunctional catalyst without the need of any additive.

Table 1. Optimization Parameters for the cycloaddition of CO_2 with styrene oxide catalyzed by **1**.[a]
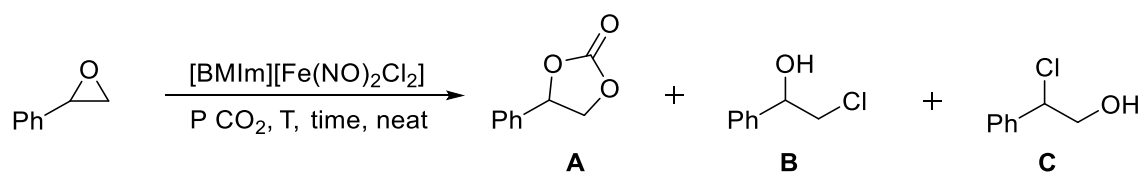
Entry	S/C (mol %)	T (ºC)	Time (h)	P (bar)	Conversion (%)[b]	Selectivity (%)[c]
1	10	R.T.	7	1	21	77 : 18 : 5
2	10	R.T.	24	1	58	85 : 12 : 3
3	10	40	24	1	>99	87 : 11 : 2
4	5	40	24	1	66	86 : 11 : 3
5	10	R.T	24	2	85	84 : 13 : 3
6	10	40	24	2	>99	83 : 13 : 3
7	**5**	**40**	**24**	**2**	**>99**	**94 : 5 : 1**
8	2.5	40	24	2	51	88 : 10 : 2
9	10	R.T.	24	3	99	76 : 21 : 3
10	10	40	24	3	>99	86 : 14 : 0
11[d]	5	40	24	2	28	70 : 24 : 6
12[e]	5	40	24	2	18	43 : 44 : 13

[a] Reagents and conditions: styrene oxide (1.665 mmol), neat, 600 rpm.[b] Conversions determined by ^1H NMR spectroscopy and refer to the selective conversion of styrene oxide (average of two runs).[c] % selectivity referred to **A** : **B** : **C**.[d] 0.0832 mmol of H_2O were added (1 equivalent regarding catalyst).[e] 1.665 mmol of H_2O were added (1 equivalent regarding substrate).

With optimized conditions in hand, a set of epoxides were tested in order to evaluate the potential of **1** as catalyst in the cycloaddition of CO_2 to oxiranes. The Fe-containing ionic liquid was found to be a highly active catalyst under very mild and near ambient conditions (Table 2). Epoxides with electron-withdrawing substituents gave higher conversions than those with electron-donor groups (entries 1-5). Indeed, the use of 1,2-epoxypentane as substrate needed higher temperatures than styrene oxide (entries 1 and 3). However, the presence of an electron-withdrawing functionality favoured the formation of **B** and led to a decrease in the chemoselectivity (entries 1 vs. 2, and 3 vs. 4), suggesting a nucleophilic attack at the Cβ of the epoxide. In addition, aliphatic epoxides required the use of higher pressures and/or temperatures than aromatic oxiranes (entries 1-5). On the other hand, the results indicate a steric influence of the substituents in the substrate, since the presence of internal and sterically hindered epoxides required the use of harder reaction conditions and led to lower conversions (entries 6 and 7). Finally, of particular interest is the cycloaddition of CO_2 to cyclohexene oxide. This transformation can be considered as a challenging one due to the steric impediment shown by the substrate. The catalytic reaction was carried out with reasonable conversion (63%) at 80 ºC and 4 bar CO_2 (entry 6), which can be considered as mild conditions.[21, 42, 52-55, 58, 59]

Table 2. Cycloaddition of CO_2 with various epoxides catalyzed by **1**.[a]

Entry	Substrate	T (°C)	P (bar)	Conv. (%)[b]	Selec. (%)[c]	TON	TOF (h⁻¹)
1	(epoxide, Ph)	40	2	>99	94 : 5 : 1	20	0.83
2	(epoxide, 4-Cl-phenyl)	40	2	>99	73 : 23 : 4	20	0.83
3	(propyl epoxide)	80	2	99	100 : 0 : 0	19.8	0.82
4	(epoxide, Cl)	80	4	>99	76 : 24 : 0	20	0.83
5	(allyl epoxide)	40	4	92	88 : 12 : 0	18.4	0.77
6	(cyclohexene oxide)	80	4	63	96 : 4 : 0	12.6	0.52
7	(epoxide, Ph, Ph)	80	4	3	100 : 0 : 0	---	---

[a] Reagents and conditions: **1** (0.0832 mmol), substrate (1.665 mmol), 24 h, neat, 600 rpm.[b] Conversions determined by ¹H NMR spectroscopy and refer to the selective conversion of epoxide (average of two runs).[c] % selectivity referred to **A** : **B** : **C**.

A key attraction to IL-based catalytic systems is the possibility of catalyst recovery and reuse. We performed an experiment employing styrene oxide as substrate in order to study the recyclability of the Fe-containing ionic liquid **1**. Through extraction of substrate and products with diethyl ether followed by re-precipitation of the insoluble fraction, complex **1** could be recovered and used in successive cycles. Nevertheless, a significant decrease in the activity was observed in the third cycle (Figure 2a), which is due to a gradual loss and/or decomposition of catalyst as a result of the repeated washing cycles. This behavior can be explained by the consumption of chloride anions associated to the formation of by-products **B** and **C**. Indeed, the recyclability was improved by the use of 1,2-epoxypentane as substrate, which does not generate chlorinated by-products. Only a slight decrease in the activity (14%) was produced after five cycles of catalyst recovery and reuse (Figure 2b), whereas the catalyst remained active in the seventh cycle and the corresponding carbonate product was obtained with 74% conversion (Figure S7, Supporting Information).
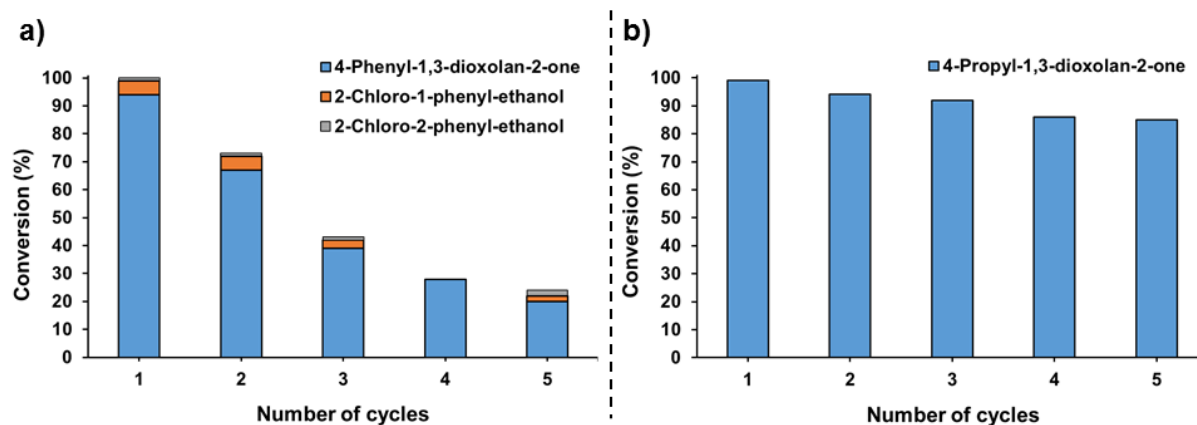
Figure 2. Reuse of **1** in the cycloaddition of CO_2 with: a) styrene oxide (reagents and conditions: **1** (5 mol %), 24 hours, 40 °C, 2 bar CO_2), and b) 1,2-epoxypentane (reagents and conditions: **1** (5 mol %), 24 hours, 80 °C, 2 bar CO_2).

1 was recovered after catalytic experiments with both substrates, and analysed by FT-IR, XPS and ionic chromatography (Cl⁻). Apart from the IR frequencies attributed to the 1-butyl-3-methyl-imidazolium cation, the FT-IR spectra (Figures S8 and S9, Supporting Information) showed the bands belonging to the NO stretching absorption (1700 and 1779 cm^{-1}), indicating the presence of NO fragments in the recovered catalysts. In addition, the high resolution XPS spectra of Fe 2p for **1** before and after catalytic experiments are very similar (Figures S6, S10b and S10d, Supporting Information). Interestingly, the high-resolution spectra of Cl 2p showed a new chloride species after reaction, consistent with simple chloride-based ionic liquids, for example [BMIm]Cl (Figures S6, S10a and S10c, Supporting Information).[89] This reveals that the initial iron-containing ionic liquid [BMIm][Fe(NO)$_2$Cl$_2$] generates the catalytically active species [BMIm][Cl] + [Fe(NO)$_2$Cl] under the reaction conditions (see *Kinetic Studies* and *Proposed Catalytic Cycle* for more details). Furthermore, ionic chromatography gave a chloride content of *ca.* 21.0% after the reaction with 1,2-epoxypentane, in good agreement with the expected value for **1** (21.75%). However, the chloride content is lower for the catalyst recovered after the experiment with styrene oxide (18.0%), due to the consumption of Cl⁻ ions related with the formation of by-products **B** and **C**. These analyses indicate that the iron-containing ionic liquid **1** evolves during the reaction, and this change is much more pronounced in the case of employing styrene oxide as substrate, since a higher amount of chlorine containing by-product is formed.

3.3. Study of the Mechanism for the Cycloaddition of CO_2 Catalyzed by [BMIm][Fe(NO)$_2$Cl$_2$]

The mechanism for the formation of cyclic carbonates *via* cycloaddition of CO_2 to epoxides was examined by experimental studies. First, a series of experiments were carried out in order to investigate the reaction mechanism and determine the importance of **1** in the catalytic process (Table 3). The imidazolium salt [BMIm]Cl and the metallic precursor [Fe(NO)$_2$Cl]$_2$ were inactive under the

optimized reaction conditions (entries 1 and 2). These results reveal that both cation and anion belonging to the Fe-based ionic liquid **1** play a role in the catalytic process, and thus proves the cooperative effect of the two fragments. Next, we found that the Fe-based ionic liquid [(n-Bu)$_4$N][Fe(NO)$_2$Cl$_2$] prepared from tetrabutylammonium chloride was less active than **1** (entries 3 and 4), which evidences the importance of the imidazolium cation to the observed catalytic activity. Similarly, the Fe-based ionic liquid [BMIm][FeCl$_4$],[90] which exhibits a different anion containing Fe and Cl, showed less activity and much less selectivity than **1** (entries 3 and 6), highlighting the role of {[Fe(NO)$_2$Cl$_2$]$^-$} moiety in the process.

Table 3. Summary of the attempted cycloaddition of CO$_2$ to oxiranes using various catalytic systems.[a]

Entry	Catalyst	Conversion (%)[b]	Selectivity (%)[c]
1	[BMIm]Cl	0	--
2	[Fe(NO)$_2$Cl]$_2$	5	0 : 0 : 100
3	[BMIm][Fe(NO)$_2$Cl$_2$]	>99	94 : 5 : 1
4	[(n-Bu)$_4$N][Fe(NO)$_2$Cl$_2$]	60	84 : 12 : 4
5	[BMMIm][Fe(NO)$_2$Cl$_2$]	59	80 : 17 : 3
6	[BMIm][FeCl$_4$]	89	65 : 24 : 11

[a] Reagents and conditions: catalyst (0.0832 mmol), styrene oxide (1.665 mmol), 24 h, neat, 40 °C, 2 bar CO$_2$, 600 rpm. [b] Conversions determined by ^{1}H NMR spectroscopy and refer to the selective conversion of styrene oxide (average of two runs). [c] % selectivity referred to **A** : **B** : **C**.

Previous mechanisms have proposed the implication of the C2 position of the imidazolium ring in the cycloaddition of CO$_2$ to oxiranes catalyzed by imidazolium-based ILs.[62, 91-96] Thus, in order to determine the influence of the H–C2 of the imidazolium cation, we prepared the Fe-based ionic liquid [BMMIm][Fe(NO)$_2$Cl$_2$] via an identical method using 1-butyl-2,3-dimethylimidazolium chloride ([BMMIm]Cl), in which this hydrogen is replaced by a methyl group. This catalyst displayed lower activity than **1** (entries 3 and 5), suggesting that the H–C2 position of the imidazolium ring is involved in the reaction mechanism, maybe through the stabilisation of anionic intermediates by H-bonding interactions. The influence of this type of hydrogen bonding interactions (CH⋯X) in the physical properties (i.e., melting point) has been described by several authors.[97-99]

In addition, the optically pure (*R*)- and (*S*)-styrene oxide were employed as substrates for the carbonate formation reaction catalyzed by **1** (Scheme 3 and Figures S11 and S12, Supporting Information). The (*R*)- and (*S*)-carbonates were obtained, respectively, with high enantioselectivity (74% and 82% *ee*, respectively). This indicates that the reaction proceeds predominantly with retention of configuration, and thus through a nucleophilic attack to the Cβ of styrene oxide, which is relatively unexpected.[100-104] Indeed, the formation of 2-chloro-1-phenylethan-1-ol (**B**) as by-product clearly demonstrates the epoxide ring opening through β attack.
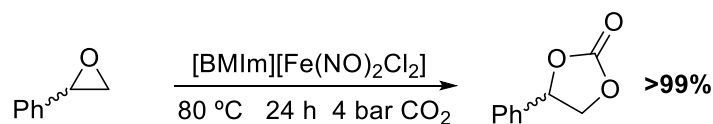
Scheme 3. Formation of optically pure carbonates by cycloaddition of CO_2 with *R*- and *S*-styrene oxide catalysed by **1**. Reagents: **1**, 0.1665 mmol; styrene oxide, 1.665 mmol. %*ee* determined by GC.

Interestingly, the reaction of the optically pure (*R*)- and (*S*)-styrene oxide with water catalyzed by **1** was mainly performed with inversion of configuration (Scheme 4 and Figures S13 and S14, Supporting Information), leading to the formation of (*S*)- and (*R*)- diol products, respectively, albeit with low-to-moderate enantioselectiviy (54% and 40% *ee*, respectively). This result points to a nucleophilic attack on the more hindered side of the epoxide (Cα) in which the nucleophile is H_2O.[105] Consequently, there could be an influence of the bulkiness of the species involved in the catalytic process, which support a role of the imidazolium moiety in the mechanism of carbonate formation. A steric effect may avoid the attack on the Cα of epoxide and direct the attack of the nucleophile on the Cβ. Nevertheless, the nucleophile is H_2O in the diol formation reaction, which does not show any steric impediment and performs the attack on the more electronically favoured Cα.[104]
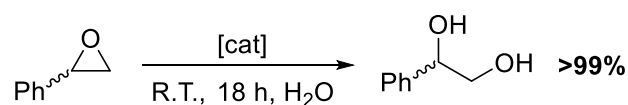
Scheme 4. Formation of diols by reaction of styrene oxide with H_2O catalyzed by **1**. Reagents: **1**, 0.1665 mmol; styrene oxide, 1.665 mmol; H_2O, 1 mL. % *ee* were determined by GC.

3.3.1. Kinetic Studies

For any reaction involving CO_2, the thermodynamics and kinetics of the process are of critical importance. If a large energy input is required, this will generate more CO_2 than is consumed by the reaction unless the process can be linked to renewable or nuclear power. However, previous studies on the experimental determination of reaction thermodynamics and kinetics for the catalytic cycloaddition of CO_2 to epoxides are scarce.[106] Theoretical calculations revealed that this transformation does not occur spontaneously because it is highly endothermic and requires a rather high activation energy (i.e., 30–60 kcal/mol).[104, 107-111] In this context, we have developed a kinetic study under solvent-free conditions in which styrene oxide served simultaneously as substrate and as solvent. Reaction kinetics at different temperatures (i.e., 40, 50, 60, 70, 80 and 90 °C) were studied and the activation energy for the process was calculated by the Arrhenius equation. The progress of these reactions was monitored by ^{1}H NMR analysis of aliquots collected at regular intervals. The apparent kinetic constant (k_{obs}) was determined by the use of the general form of the

rate equation given by equation (1) and equation (2).[106] Analysis of the reaction kinetics revealed that the process followed first-order kinetics regarding epoxide concentration (Figure S16, Supporting Information), whereas CO_2 gas (present in large excess with a gas reservoir) and the concentration of [BMIm][Fe(NO)$_2$Cl$_2$] were assumed to remain effectively constant during the process.

$$r = k \, [\text{epoxide}]^a [CO_2]^b [[\text{BMIm}][\text{Fe(NO)}_2\text{Cl}_2]]^c \qquad \text{(Eq. 1)}$$

$$r = k_{obs}[\text{epoxide}]^a, \, where \, k_{obs} = k[CO_2]^b[[\text{BMIm}][\text{Fe(NO)}_2\text{Cl}_2]]^c \qquad \text{(Eq. 2)}$$

$$\ln (k_{obs}) = \ln(A) - \frac{E_{a-app}}{R}\left(\frac{1}{T}\right) \qquad \text{(Eq. 3)}$$

By varying the CO_2 pressure (constant pressure of 2, 4 and 6 bar maintained with a gas reservoir, see figure S15a) and [BMIm][Fe(NO)$_2$Cl$_2$] concentration (2.5, 5.0 and 7.5% mol/mol epoxide, see figure S15b), but maintaining all the other parameters constant (substrate concentration and temperature), the order of reaction for CO_2 and [BMIm][Fe(NO)$_2$Cl$_2$] was determined to be zero and 1.5, respectively.[106] The zero–order dependence on CO_2 concentration is attributable to the large excess of gas present in solution due to the high solubility of CO_2 in the IL medium, while the 1.5–order dependence on the [BMIm][Fe(NO)$_2$Cl$_2$] catalyst concentration exhibited by the rate was unexpected and indicates that 1.5 separate molecules of [BMIm][Fe(NO)$_2$Cl$_2$] are involved in the catalytic cycle before the rate-determining step. It was also noted that reactions carried out at very low concentration of [BMIm][Fe(NO)$_2$Cl$_2$] showed an induction period. Furthermore, a deactivation of the catalyst was observed in some catalytic experiments by the formation of chlorinated products derived from the epoxide aperture by chloride anion nucleophilic attack. However, this was not apparent in reactions carried out at higher concentrations of [BMIm][Fe(NO)$_2$Cl$_2$]. An analogous behavior was recently described for the same process mediated by Al-Lewis Acid catalysts dissolved in tetrabutylammonium bromide ILs.[106]

This dependence on the [BMIm][Fe(NO)$_2$Cl$_2$] concentration was correlated with the fact that two reaction regimes were observed in the Arrhenius plot (Figure 3): one regime with Ea = 321 Kcal/mol at low-to-mild temperature (i.e., 40 to 60 °C), and another one with Ea = 31 Kcal/mol at mild-to-high temperatures (i.e., 70 to 90 °C). The presence of these two regimes suggests the existence of a fast pre-equilibrium, as it was previously observed for enzymatic systems with non-reactive (NR) and reactive (R) states.[112] This reversible pre-equilibrium determines the concentration of non-reactive (NR) and reactive (R) species in the reaction medium (i.e., NR ⇔ R, and K = [R]/[NR]), that is, the fast pre-equilibrium governs the reaction rate. Thus, the dissociated species corresponding to the reactive state predominate at high temperature, whereas the non-reactive state predominates at low temperature, and the reaction partners (i.e., [BMIm][Fe(NO)$_2$Cl$_2$] ⇔ [BMIm][Cl] + [Fe(NO)$_2$Cl]) are immersed in strong interactions with other species. This observation is very important to address the

nature of the true-catalytically active species and understand the reaction mechanism that takes place with iron-chloride anions dissolved in ILs.
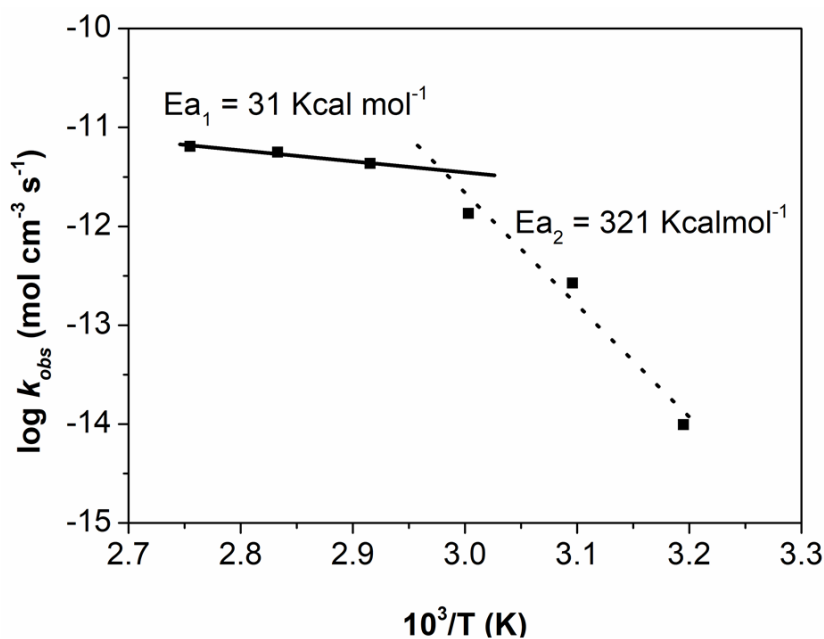

Figure 3. Arrhenius plot for the cycloaddition reaction of CO_2 with styrene oxide catalyzed by **1**.

3.3.2. Proposed Catalytic Cycle

Two mechanisms are possible under the optimal reaction conditions. The first possibility is the reaction mechanism proposed for catalysts bearing good nucleophile and good leaving groups (i.e., bromide and iodide salts): (a) ring opening of the epoxide by the nucleophile with the formation of an alkoxide, (b) reaction of the alkoxide with CO_2 to give a carbonate, and (c) intramolecular displacement of the nucleophile by the carbonate to yield the five-membered ring and regenerate the catalyst.[110, 113] Alternatively, the reaction pathways observed for systems bearing a Lewis acidic metal-based catalyst (i.e., Co-MOF[111] and Zn-Salphen[104]) could also act under our mild reaction conditions: (a) activation of epoxide by the Lewis acidic metal-based catalyst and formation of a primary radical through cleavage of the less substituted C–O bond, and (b) CO_2 binding with the primary radical complex and carbonate formation by cyclization through a five-membered cyclic transition state. The radical mechanism was examined by free-radical termination experiments under the reaction conditions. Different free radical scavengers, such as galvinoxyl and 1,1-diphenyl-2-picrylhydrazyl (DPPH),[111] were added to the mixture of the cycloaddition reaction of CO_2 with styrene oxide catalyzed by [BMIm][Fe(NO)$_2$Cl$_2$]. The catalytic reaction in the presence of either galvinoxyl or DPPH still led to the formation of desired product with moderate to good conversions (galvinoxyl: 91% conversion and 81% selectivity; DPPH: 74% conversion and 41% selectivity). Therefore, a radical mechanism can be dismissed as the catalytic pathway.

The catalytic system described herein could be considered as a combination of these two types of catalyst. The Lewis acidic Fe-site is combined with a chloride anion, allowing the carbonate formation under mild conditions. The aim is to identify the nature of the true-catalytically active species, i.e., [BMIm][Fe(NO)$_2$Cl$_2$] $\Leftrightarrow$ [BMIm]$^+$[Cl]$^-$ + [Fe(NO)$_2$Cl]. The experimental kinetic data suggests that [BMIm]$^+$[Cl]$^-$ ([Cl]$^-$ acting as nucleophile) and [Fe(NO)$_2$Cl] (Fe acting as Lewis acid) are the true-catalytically reactive state, and the [BMIm][Fe(NO)$_2$Cl$_2$] is the non-reactive state.
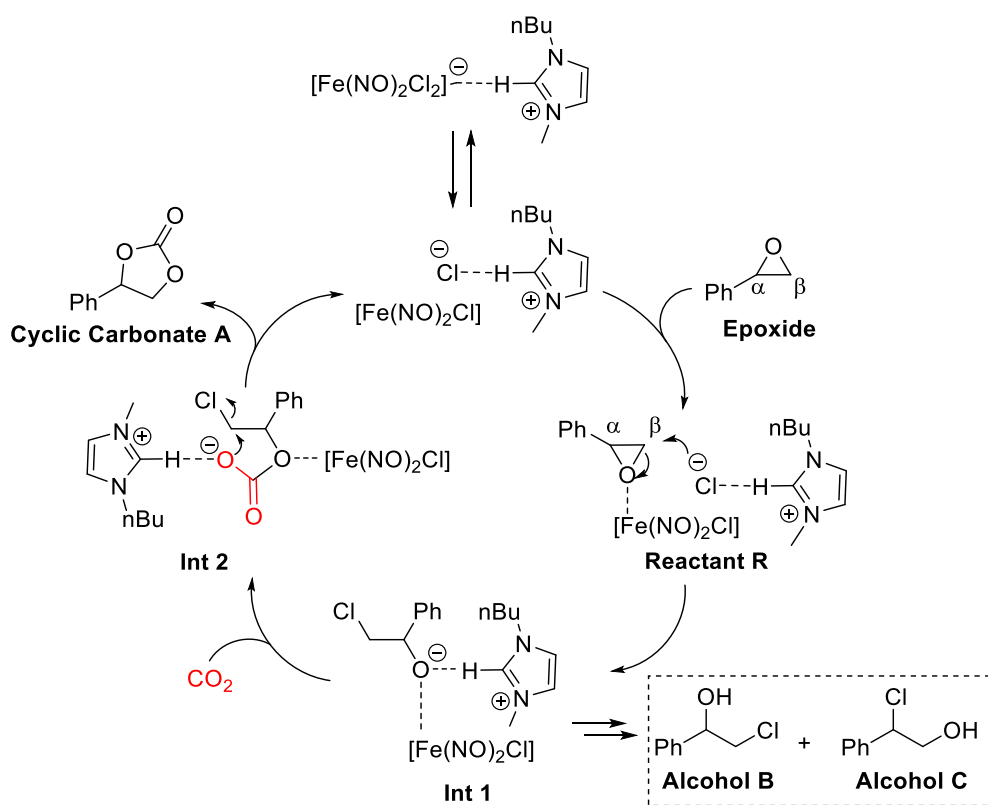
Scheme 5. Proposed catalytic cycle for the formation of carbonates catalyzed by **1**.

On the basis of the experimental evidences, we proposed the catalytic cycle depicted in Scheme 5, which is also supported by state-of-the-art DFT calculations that are focused upon similar Lewis acidic systems.[114, 115] After activation of the epoxide through coordination with the Lewis acid [Fe(NO)$_2$Cl], the nucleophilic attack of [BMIm]Cl on the epoxide promotes a ring opening reaction and the formation of the alkoxide intermediate (**Int1**). This nucleophilic attack is favored on the less sterically-hindered Cβ, as is demonstrated by two facts: (1) alcohol by-product **B** is formed in much higher ratio than alcohol byproduct **C**, and (2) when the optically pure epoxide was employed as substrate, the configuration of the obtained cyclic carbonate was retained and only a slight decrease of the enantioselectivity was observed. In addition, the interaction of H–C2 of imidazolium ring with the substrate *via* H-bonding in **Int1** is supported through the reactions catalyzed by [BMMIm][Fe(NO)$_2$Cl$_2$] and [(*n*-Bu)$_4$N][Fe(NO)$_2$Cl$_2$] (1-butyl-2,3-dimethylimidazolium and

tetrabutylammonium cations, respectively), which showed lower reaction rates. Next, the insertion of CO_2 into the **Int1** and the following ring closure by nucleophilic attack of the carbonate to the C–Cl bond affords the cyclic carbonate and regenerate the catalyst. To the best of our knowledge, this is the first case which describes the formation of alcohols **B** and **C** as byproducts by protonation of the alkoxide under the near-ambient reaction conditions employed herein (2 bar and 40 ℃). We tried to avoid the formation of **B** and **C** by increasing the temperature to 80 ℃ in the catalytic reactions with styrene oxide and *p*-chlorostyrene oxide, but the corresponding carbonate products were formed with identical selectivities as those observed at 40 ℃ (Table 3, entries 1 and 2). Furthermore, we performed the cycloaddition of carbon dioxide to **B** catalyzed by **1** in order to study the implication of this by-product as intermediate in the catalytic cycle. However, no reaction was observed. Therefore, the by-products are formed through a deactivation pathway and they could be considered as a kind of very stable dormant catalytic species, since the chloride nucleophile is trapped into their structures and, consequently, the decrease in the activity observed after each run during the recycling experiment with styrene oxide can be attributed to the loss of [Cl$^-$] nucleophile. Indeed, the catalyst remained active in the seventh cycle by the use of 1,2-epoxypentane as substrate, which does not generate such by-products. The formation of these byproducts is favored for epoxides with electron-withdrawing substituents due to the higher basicity of the generated alkoxide.[116]

4. Conclusions

In this work, we report key studies for the understanding of the reaction mechanism of the cycloaddition of CO_2 to epoxides catalysed by metal-containing ionic liquids. For this purpose, we have successfully used the dimer [Fe(NO)$_2$Cl]$_2$ as metallic precursor for the synthesis of the imidazolium based iron-containing ionic liquid [BMIm][Fe(NO)$_2$Cl$_2$]. An extensive characterization was performed by a wide variety of techniques, which enabled us to propose this structure for the iron-based containing ionic liquid. This system was found to be a highly active catalyst for the cycloaddition of CO_2 to oxiranes, giving high conversions and chemoselectivities under near ambient conditions and without the need of any additive. Furthermore, the catalytic system showed a good recycling performance and the catalyst remained active in the seventh cycle of recovery and reuse.

The complex works as a bifunctional catalyst playing a crucial double role, as Lewis acid and as nucleophile. In addition to the catalytic studies, the reaction mechanism and the nature of the different species involved in the catalytic cycle of this transformation was interrogated by experimental studies. Such experiments demonstrated that the imidazolium moiety is involved in the catalytic process, whereas the reaction proceeds with retention of configuration through a nucleophilic attack to the Cβ of the epoxide. In addition, kinetic studies showed that the process followed first-order kinetics regarding epoxide concentration and revealed the presence of a fast reversible pre-equilibrium in which the iron-containing ionic liquid [BMIm][Fe(NO)$_2$Cl$_2$] (non-reactive state) dissociates at high temperature and generates the true-catalytically active species, [BMIm][Cl] + [Fe(NO)$_2$Cl].

On the basis of these experiments, a catalytic cycle was proposed. The [Fe(NO)$_2$Cl] fragment operates as Lewis acid leading to the activation of the epoxide, whereas the chloride [Cl]$^-$, as part of [BMIm][Cl] moiety, acts as nucleophile and promotes the ring opening of substrate through a nucleophilic attack on the less sterically-hindered Cβ. Interestingly, experimental evidences demonstrated that the process is favoured by an interaction *via* H-bonding between the substrate and the H–C2 of imidazolium ring. In conclusion we may say that with the study reported herein, we have elucidated the nature of the true-catalytically active species involved in the cycloaddition of CO$_2$ to oxiranes mediated by iron-containing ionic liquids.

Acknowledgements

Appendix A. Supplementary data

Supporting information: detailed synthetic procedures, kinetic experiments, recycling experiment, GC chromatograms, analytical and spectral data. Supplementary data associated with this article can be found, in the online version.

Notes and References

[1] M. Aresta, A. Dibenedetto, I. Tommasi, Developing Innovative Synthetic Technologies of Industrial Relevance Based on Carbon Dioxide as Raw Material, Energy Fuels, 15 (2001) 269-273.
[2] I. Omae, Aspects of carbon dioxide utilization, Catal. Today, 115 (2006) 33-52.
[3] T. Sakakura, J.-C. Choi, H. Yasuda, Transformation of Carbon Dioxide, Chem. Rev., 107 (2007) 2365-2387.
[4] M. Aresta, Carbon Dioxide: Utilization Options to Reduce its Accumulation in the Atmosphere, Carbon Dioxide as Chemical Feedstock, Wiley-VCH Verlag GmbH & Co. KGaA 2010, pp. 1-13.
[5] A.J. Hunt, E.H.K. Sin, R. Marriott, J.H. Clark, Generation, Capture, and Utilization of Industrial Carbon Dioxide, ChemSusChem, 3 (2010) 306-322.
[6] M. Peters, B. Köhler, W. Kuckshinrichs, W. Leitner, P. Markewitz, T.E. Müller, Chemical Technologies for Exploiting and Recycling Carbon Dioxide into the Value Chain, ChemSusChem, 4 (2011) 1216-1240.
[7] G. Centi, G. Iaquaniello, S. Perathoner, Can We Afford to Waste Carbon Dioxide? Carbon Dioxide as a Valuable Source of Carbon for the Production of Light Olefins, ChemSusChem, 4 (2011) 1265-1273.
[8] N.S. Spinner, J.A. Vega, W.E. Mustain, Recent progress in the electrochemical conversion and utilization of CO$_2$, Catal. Sci. Technol., 2 (2012) 19-28.
[9] G.A. Olah, Towards Oil Independence Through Renewable Methanol Chemistry, Angew. Chem. Int. Ed., 52 (2013) 104-107.

[10] M. Aresta, A. Dibenedetto, E. Quaranta, State of the art and perspectives in catalytic processes for CO_2 conversion into chemicals and fuels: The distinctive contribution of chemical catalysis and biotechnology, J. Catal., 343 (2016) 2-45.

[11] J. Klankermayer, S. Wesselbaum, K. Beydoun, W. Leitner, Selective Catalytic Synthesis Using the Combination of Carbon Dioxide and Hydrogen: Catalytic Chess at the Interface of Energy and Chemistry, Angew. Chem. Int. Ed., 55 (2016) 7296-7343.

[12] H.A. Patel, J. Byun, C.T. Yavuz, Carbon Dioxide Capture Adsorbents: Chemistry and Methods, ChemSusChem, 10 (2017) 1303-1317.

[13] T.P. Senftle, E.A. Carter, The Holy Grail: Chemistry Enabling an Economically Viable CO_2 Capture, Utilization, and Storage Strategy, Acc. Chem. Res., 50 (2017) 472-475.

[14] H. Yoshida, H. Fukushima, J. Ohshita, A. Kunai, CO_2 Incorporation Reaction Using Arynes: Straightforward Access to Benzoxazinone, J. Am. Chem. Soc., 128 (2006) 11040-11041.

[15] S. Das, F.D. Bobbink, G. Laurenczy, P.J. Dyson, Metal-Free Catalyst for the Chemoselective Methylation of Amines Using Carbon Dioxide as a Carbon Source, Angew. Chem. Int. Ed., 53 (2014) 12876-12879.

[16] A. Tlili, E. Blondiaux, X. Frogneux, T. Cantat, Reductive functionalization of CO_2 with amines: an entry to formamide, formamidine and methylamine derivatives, Green Chem., 17 (2015) 157-168.

[17] X. Frogneux, E. Blondiaux, P. Thuéry, T. Cantat, Bridging Amines with CO_2: Organocatalyzed Reduction of CO_2 to Aminals, ACS Catal., 5 (2015) 3983-3987.

[18] Q. Liu, L. Wu, R. Jackstell, M. Beller, Using carbon dioxide as a building block in organic synthesis, Nature Commun., 6 (2015) 5933-5948.

[19] D.J. Darensbourg, M.W. Holtcamp, Catalysts for the reactions of epoxides and carbon dioxide, Coord. Chem. Rev., 153 (1996) 155-174.

[20] T. Sakakura, K. Kohno, The synthesis of organic carbonates from carbon dioxide, Chem. Commun., (2009) 1312-1330.

[21] M. North, R. Pasquale, C. Young, Synthesis of cyclic carbonates from epoxides and CO_2, Green Chem., 12 (2010) 1514-1539.

[22] R. Martín, A.W. Kleij Myth or Reality? Fixation of Carbon Dioxide into Complex Organic Matter under Mild Conditions, ChemSusChem, 4 (2011) 1259-1263.

[23] N. Kielland, C.J. Whiteoak, A.W. Kleij, Stereoselective Synthesis with Carbon Dioxide, Adv. Synth. Catal., 355 (2013) 2115-2138.

[24] C. Martín, G. Fiorani, A.W. Kleij, Recent Advances in the Catalytic Preparation of Cyclic Organic Carbonates, ACS Catal., 5 (2015) 1353-1370.

[25] C.J. Whiteoak, A.W. Kleij, Catalyst Development in the Context of Ring Expansion–Addition of Carbon Dioxide to Epoxides to Give Organic Carbonates, Synlett, 24 (2013) 1748-1756.

[26] J.H. Clements, Reactive Applications of Cyclic Alkylene Carbonates, Ind. Eng. Chem. Res., 42 (2003) 663-674.

[27] K. Xu, Nonaqueous Liquid Electrolytes for Lithium-Based Rechargeable Batteries, Chem. Rev., 104 (2004) 4303-4418.

[28] D.J. Darensbourg, Making Plastics from Carbon Dioxide: Salen Metal Complexes as Catalysts for the Production of Polycarbonates from Epoxides and CO_2, Chem. Rev., 107 (2007) 2388-2410.

[29] B. Schäffner, F. Schäffner, S.P. Verevkin, A. Börner, Organic Carbonates as Solvents in Synthesis and Catalysis, Chem. Rev., 110 (2010) 4554-4581.

[30] V. Etacheri, R. Marom, R. Elazari, G. Salitra, D. Aurbach, Challenges in the development of advanced Li-ion batteries: a review, Energy Environ. Sci, 4 (2011) 3243-3262.

[31] C. Beattie, M. North, P. Villuendas, Proline-Catalysed Amination Reactions in Cyclic Carbonate Solvents, Molecules, 16 (2011).

[32] L.-N. He, H. Yasuda, T. Sakakura, New procedure for recycling homogeneous catalyst: propylene carbonate synthesis under supercritical CO_2 conditions, Green Chem., 5 (2003) 92-94.

[33] J.-W. Huang, M. Shi, Chemical Fixation of Carbon Dioxide by $NaI/PPh_3/PhOH$, J. Org. Chem., 68 (2003) 6705-6709.

[34] H. Kawanami, Y. Ikushima, Chemical fixation of carbon dioxide to styrene carbonate under supercritical conditions with DMF in the absence of any additional catalysts, Chem. Commun., (2000) 2089-2090.

[35] Y.-M. Shen, W.-L. Duan, M. Shi, Phenol and Organic Bases Co-Catalyzed Chemical Fixation of Carbon Dioxide with Terminal Epoxides to Form Cyclic Carbonates, Adv. Synth. Catal., 345 (2003) 337-340.

[36] G. Fiorani, W. Guo, A.W. Kleij, Sustainable conversion of carbon dioxide: the advent of organocatalysis, Green Chem., 17 (2015) 1375-1389.

[37] N. Kihara, N. Hara, T. Endo, Catalytic activity of various salts in the reaction of 2,3-epoxypropyl phenyl ether and carbon dioxide under atmospheric pressure, J. Org. Chem., 58 (1993) 6198-6202.

[38] T. Yano, H. Matsui, T. Koike, H. Ishiguro, H. Fujihara, M. Yoshihara, T. Maeshima, Magnesium oxide-catalysed reaction of carbon dioxide with an epoxide with retention of stereochemistry, Chem. Commun., (1997) 1129-1130.

[39] K. Yamaguchi, K. Ebitani, T. Yoshida, H. Yoshida, K. Kaneda, Mg−Al Mixed Oxides as Highly Active Acid−Base Catalysts for Cycloaddition of Carbon Dioxide to Epoxides, J. Am. Chem. Soc., 121 (1999) 4526-4527.

[40] A. Decortes, A.M. Castilla, A.W. Kleij, Salen-Complex-Mediated Formation of Cyclic Carbonates by Cycloaddition of CO_2 to Epoxides, Angew. Chem. Int. Ed., 49 (2010) 9822-9837.

[41] X.-B. Lu, D.J. Darensbourg, Cobalt catalysts for the coupling of CO_2 and epoxides to provide polycarbonates and cyclic carbonates, Chem. Soc. Rev., 41 (2012) 1462-1484.

[42] Y. Chen, R. Qiu, X. Xu, C.-T. Au, S.-F. Yin, Organoantimony and organobismuth complexes for CO_2 fixation, RSC Adv., 4 (2014) 11907-11918.

[43] F. de la Cruz-Martínez, J. Martínez, M.A. Gaona, J. Fernández-Baeza, L.F. Sánchez-Barba, A.M. Rodríguez, J.A. Castro-Osma, A. Otero, A. Lara-Sánchez, Bifunctional Aluminum Catalysts for the Chemical Fixation of Carbon Dioxide into Cyclic Carbonates, ACS Sustainable Chem. Eng., 6 (2018) 5322-5332.

[44] D.O. Meléndez, A. Lara-Sánchez, J. Martínez, X. Wu, A. Otero, J.A. Castro-Osma, M. North, R.S. Rojas, Amidinate Aluminium Complexes as Catalysts for Carbon Dioxide Fixation into Cyclic Carbonates, ChemCatChem, 10 (2018) 2271-2277.

[45] C.M. Miralda, E.E. Macias, M. Zhu, P. Ratnasamy, M.A. Carreon, Zeolitic Imidazole Framework-8 Catalysts in the Conversion of CO_2 to Chloropropene Carbonate, ACS Catal., 2 (2012) 180-183.

[46] M. Zhu, D. Srinivas, S. Bhogeswararao, P. Ratnasamy, M.A. Carreon, Catalytic activity of ZIF-8 in the synthesis of styrene carbonate from CO_2 and styrene oxide, Catal. Commun., 32 (2013) 36-40.

[47] J. Liang, Y.-Q. Xie, X.-S. Wang, Q. Wang, T.-T. Liu, Y.-B. Huang, R. Cao, An imidazolium-functionalized mesoporous cationic metal–organic framework for cooperative CO_2 fixation into cyclic carbonate, Chem. Commun., 54 (2018) 342-345.

[48] D.-H. Lan, L. Chen, C.-T. Au, S.-F. Yin, One-pot synthesized multi-functional graphene oxide as a water-tolerant and efficient metal-free heterogeneous catalyst for cycloaddition reaction, Carbon, 93 (2015) 22-31.

[49] D.-H. Lan, H.-T. Wang, L. Chen, C.-T. Au, S.-F. Yin, Phosphorous-modified bulk graphitic carbon nitride: Facile preparation and application as an acid-base bifunctional and efficient catalyst for CO_2 cycloaddition with epoxides, Carbon, 100 (2016) 81-89.

[50] D.-H. Lan, Y.-X. Gong, N.-Y. Tan, S.-S. Wu, J. Shen, K.-C. Yao, B. Yi, C.-T. Au, S.-F. Yin, Multi-functionalization of GO with multi-cationic ILs as high efficient metal-free catalyst for CO_2 cycloaddition under mild conditions, Carbon, 127 (2018) 245-254.

[51] D.-H. Lan, F.-M. Yang, S.-L. Luo, C.-T. Au, S.-F. Yin, Water-tolerant graphene oxide as a high-efficiency catalyst for the synthesis of propylene carbonate from propylene oxide and carbon dioxide, Carbon, 73 (2014) 351-360.

[52] J. Sun, S.-i. Fujita, M. Arai, Development in the green synthesis of cyclic carbonate from carbon dioxide using ionic liquids, J. Organomet. Chem., 690 (2005) 3490-3497.

[53] L. Yang, H. Wang, Recent Advances in Carbon Dioxide Capture, Fixation, and Activation by using N-Heterocyclic Carbenes, ChemSusChem, 7 (2014) 962-998.

[54] B.-H. Xu, J.-Q. Wang, J. Sun, Y. Huang, J.-P. Zhang, X.-P. Zhang, S.-J. Zhang, Fixation of CO_2 into cyclic carbonates catalyzed by ionic liquids: a multi-scale approach, Green Chem., 17 (2015) 108-122.

[55] F.D. Bobbink, P.J. Dyson, Synthesis of carbonates and related compounds incorporating CO_2 using ionic liquid-type catalysts: State-of-the-art and beyond, J. Catal., 343 (2016) 52-61.

[56] D.-H. Lan, N. Fan, Y. Wang, X. Gao, P. Zhang, L. Chen, C.-T. Au, S.-F. Yin, Recent advances in metal-free catalysts for the synthesis of cyclic carbonates from CO_2 and epoxides, Chin. J. Catal., 37 (2016) 826-845.

[57] Q. He, J.W. O'Brien, K.A. Kitselman, L.E. Tompkins, G.C.T. Curtis, F.M. Kerton, Synthesis of cyclic carbonates from CO_2 and epoxides using ionic liquids and related catalysts including choline chloride–metal halide mixtures, Catal. Sci. Technol., 4 (2014) 1513-1528.

[58] Z.-Z. Yang, Y.-N. Zhao, L.-N. He, CO_2 chemistry: task-specific ionic liquids for CO_2 capture/activation and subsequent conversion, RSC Adv., 1 (2011) 545-567.

[59] W. Cheng, Q. Su, J. Wang, J. Sun, F. Ng, Ionic Liquids: The Synergistic Catalytic Effect in the Synthesis of Cyclic Carbonates, Catalysts, 3 (2013) 878-901.

[60] M.S. Sitze, E.R. Schreiter, E.V. Patterson, R.G. Freeman, Ionic Liquids Based on $FeCl_3$ and $FeCl_2$. Raman Scattering and ab Initio Calculations, Inorg. Chem., 40 (2001) 2298-2304.

[61] A.P. Abbott, G. Frisch, K.S. Ryder, Metal complexation in ionic liquids, Annual Reports on the Progress of Chemistry, Section A: Inorganic Chemistry, 104 (2008) 21-45.

[62] J. Gao, Q.-W. Song, L.-N. He, C. Liu, Z.-Z. Yang, X. Han, X.-D. Li, Q.-C. Song, Preparation of polystyrene-supported Lewis acidic Fe(III) ionic liquid and its application in catalytic conversion of carbon dioxide, Tetrahedron, 68 (2012) 3835-3842.

[63] L. Han, M.-S. Park, S.-J. Choi, Y.-J. Kim, S.-M. Lee, D.-W. Park, Incorporation of Metal Ions into Silica-Grafted Imidazolium-Based Ionic Liquids to Efficiently Catalyze Cycloaddition Reactions of CO_2 and Epoxides, Catal. Lett., 142 (2012) 259-266.

[64] M.-I. Kim, S.-J. Choi, D.-W. Kim, D.-W. Park, Catalytic performance of zinc containing ionic liquids immobilized on silica for the synthesis of cyclic carbonates, J. Ind. Eng. Chem., 20 (2014) 3102-3107.

[65] D. Kim, Y. Moon, D. Ji, H. Kim, D. Cho, Metal-Containing Ionic Liquids as Synergistic Catalysts for the Cycloaddition of CO_2: A Density Functional Theory and Response Surface Methodology Corroborated Study, ACS Sustainable Chem. Eng., 4 (2016) 4591-4600.

[66] W.L.F. Armarego, D.D. Perrin, Purification of Laboratory Chemicals, Butterworth-Heineman, Oxford (UK), 1997.

[67] A.W. Taylor, S. Men, C.J. Clarke, P. Licence, Acidity and basicity of halometallate-based ionic liquids from X-ray photoelectron spectroscopy, RSC Adv., 3 (2013) 9436-9445.

[68] J. Dupont, C.S. Consorti, P.A.Z. Suarez, R.F.d. Souza, Preparation of 1-Butyl-3-Methyl Imidazolium-Based Room Temperature Ionic Liquids, Org. Synth., 79 (2002) 236-240.

[69] D. Ballivet-Tkatchenko, B. Nickel, A. Rassat, J. Vincent-Vaucquelin, Cationic metal nitrosyl complexes. 6. Characterization of the 19-electron iron nitrosyl radical cation [Fe(NO)2LL'2]+, Inorg. Chem., 25 (1986) 3497-3501.

[70] Unfortunately, no helpful information can be extracted from the ESI-MS spectrum in the negative mode and only one peak corresponding to the [Fe(NO)Cl$_2$] species could be identified.

[71] T.W. Hayton, P. Legzdins, W.B. Sharp, Coordination and Organometallic Chemistry of Metal−NO Complexes, Chem. Rev., 102 (2002) 935-992.

[72] T.C. Berto, A.L. Speelman, S. Zheng, N. Lehnert, Mono- and dinuclear non-heme iron–nitrosyl complexes: Models for key intermediates in bacterial nitric oxide reductases, Coord. Chem. Rev., 257 (2013) 244-259.

[73] Z.J. Tonzetich, L.H. Do, S.J. Lippard, Dinitrosyl Iron Complexes Relevant to Rieske Cluster Nitrosylation, J. Am. Chem. Soc., 131 (2009) 7964-7965.

[74] C.T. Tran, E. Kim, Acid-dependent degradation of a [2Fe-2S] cluster by nitric oxide, Inorg. Chem., 51 (2012) 10086-10088.

[75] C.A. Brown, M.A. Pavlosky, T.E. Westre, Y. Zhang, B. Hedman, K.O. Hodgson, E.I. Solomon, Spectroscopic and Theoretical Description of the Electronic Structure of S = 3/2 Iron-Nitrosyl Complexes and Their Relation to O_2 Activation by Non-Heme Iron Enzyme Active Sites, J. Am. Chem. Soc., 117 (1995) 715-732.

[76] T.E. Westre, A. Di Cicco, A. Filipponi, C.R. Natoli, B. Hedman, E.I. Solomon, K.O. Hodgson, Determination of the Fe-N-O Angle in {FeNO}[7] Complexes Using Multiple-Scattering EXAFS Analysis by GNXAS, J. Am. Chem. Soc., 116 (1994) 6757-6768.

[77] C. Hauser, T. Glaser, E. Bill, T. Weyhermüller, K. Wieghardt, The Electronic Structures of an Isostructural Series of Octahedral Nitrosyliron Complexes $\{Fe-NO\}^{6,7,8}$ Elucidated by Mössbauer Spectroscopy, J. Am. Chem. Soc., 122 (2000) 4352-4365.

[78] A. Wanat, T. Schneppensieper, G. Stochel, R. van Eldik, E. Bill, K. Wieghardt, Kinetics, Mechanism, and Spectroscopy of the Reversible Binding of Nitric Oxide to Aquated Iron(II). An Undergraduate Text Book Reaction Revisited, Inorg. Chem., 41 (2002) 4-10.

[79] S. Begel, R. Puchta, J. Sutter, F.W. Heinemann, L. Dahlenburg, R. Eldik, Studies on the Reaction of Iron(II) with NO in a Noncoordinating Ionic Liquid, Inorg. Chem., 54 (2015) 6763-6775.

[80] I. de Pedro, O. Fabelo, A. Garcia-Saiz, O. Vallcorba, J. Junquera, J.A. Blanco, J.C. Waerenborgh, D. Andreica, A. Wildes, M.T. Fernandez-Diaz, J.R. Fernandez, Dynamically slow solid-to-solid phase transition induced by thermal treatment of DimimFeCl$_4$ magnetic ionic liquid, Phys. Chem. Chem. Phys., 18 (2016) 21881-21892.

[81] I. de Pedro, A. García-Saiz, J. González, I. Ruiz de Larramendi, T. Rojo, C.A.M. Afonso, S.P. Simeonov, J.C. Waerenborgh, J.A. Blanco, B. Ramajo, J.R. Fernández, Magnetic ionic plastic crystal: choline[FeCl$_4$], Phys. Chem. Chem. Phys., 15 (2013) 12724-12733.

[82] A. Garcia-Saiz, I. de Pedro, J.A. Blanco, J. Gonzalez, J. Rodriguez Fernandez, Pressure effects on Emim[FeCl$_4$], a magnetic ionic liquid with three-dimensional magnetic ordering, J. Phys. Chem. B, 117 (2013) 3198-3206.

[83] A. Garcia-Saiz, I. de Pedro, P. Migowski, O. Vallcorba, J. Junquera, J.A. Blanco, O. Fabelo, D. Sheptyakov, J.C. Waerenborgh, M.T. Fernandez-Diaz, J. Rius, J. Dupont, J.A. Gonzalez, J.R. Fernandez, Anion-pi and halide-halide nonbonding interactions in a new ionic liquid based on imidazolium cation with three-dimensional magnetic ordering in the solid state, Inorg. Chem., 53 (2014) 8384-8396.

[84] A. García-Saiz, I. de Pedro, O. Vallcorba, P. Migowski, I. Hernández, L. Fernández Barquin, I. Abrahams, M. Motevalli, J. Dupont, J.A. Gonzalez, J.R. Fernández, 1-Ethyl-2,3-dimethylimidazolium paramagnetic ionic liquids with 3D magnetic ordering in its solid state: synthesis, structure and magneto-structural correlations, RSC Adv., 5 (2015) 60835-60848.

[85] L. Wang, C. Guo, Y. Zhu, J. Zhou, L. Fan, Y. Qian, A FeCl$_2$-graphite sandwich composite with Cl doping in graphite layers: a new anode material for high-performance Li-ion batteries, Nanoscale, 6 (2014) 14174-14179.

[86] Z. Beji, M. Sun, L.S. Smiri, F. Herbst, C. Mangeney, S. Ammar, Polyol synthesis of non-stoichiometric Mn-Zn ferrite nanocrystals: structural /microstructural characterization and catalytic application, RSC Adv., 5 (2015) 65010-65022.

[87] M.I. Qadir, A. Weilhard, J.A. Fernandes, I. de Pedro, B.J.C. Vieira, J.C. Waerenborgh, J. Dupont, Selective Carbon Dioxide Hydrogenation Driven by Ferromagnetic RuFe Nanoparticles in Ionic Liquids, ACS Catal., 8 (2018) 1621-1627.

[88] Once the reaction was finished, diethyl ether was employed for the extraction of products.

[89] I.J. Villar-Garcia, E.F. Smith, A.W. Taylor, F. Qiu, K.R.J. Lovelock, R.G. Jones, P. Licence, Charging of ionic liquid surfaces under X-ray irradiation: the measurement of absolute binding energies by XPS, Phys. Chem. Chem. Phys., 13 (2011) 2797-2808.

[90] H. Wang, R. Yan, Z. Li, X. Zhang, S. Zhang, Fe-containing magnetic ionic liquid as an effective catalyst for the glycolysis of poly(ethylene terephthalate), Catal. Commun., 11 (2010) 763-767.

[91] Y.J. Kim, R.S. Varma, Tetrahaloindate(III)-Based Ionic Liquids in the Coupling Reaction of Carbon Dioxide and Epoxides To Generate Cyclic Carbonates: H-Bonding and Mechanistic Studies, J. Org. Chem., 70 (2005) 7882-7891.

[92] F. Li, L. Xiao, C. Xia, B. Hu, Chemical fixation of CO_2 with highly efficient ZnCl$_2$/[BMIm]Br catalyst system, Tetrahedron Lett., 45 (2004) 8307-8310.

[93] G. Gurau, H. Rodríguez, S.P. Kelley, P. Janiczek, R.S. Kalb, R.D. Rogers, Demonstration of Chemisorption of Carbon Dioxide in 1,3-Dialkylimidazolium Acetate Ionic Liquids, Angew. Chem. Int. Ed., 50 (2011) 12024-12026.

[94] O. Holloczki, D. Gerhard, K. Massone, L. Szarvas, B. Nemeth, T. Veszpremi, L. Nyulaszi, Carbenes in ionic liquids, New J. Chem., 34 (2010) 3004-3009.

[95] M. Besnard, M.I. Cabaço, F. Vaca Chávez, N. Pinaud, P.J. Sebastião, J.A.P. Coutinho, J. Mascetti, Y. Danten, CO_2 in 1-Butyl-3-methylimidazolium Acetate. 2. NMR Investigation of Chemical Reactions, J. Phys. Chem. A, 116 (2012) 4890-4901.

[96] J. Blath, N. Deubler, T. Hirth, T. Schiestel, Chemisorption of carbon dioxide in imidazolium based ionic liquids with carboxylic anions, Chem. Eng. J., 181-182 (2012) 152-158.

[97] A.a.K. Abdul-Sada, A.M. Greenway, P.B. Hitchcock, T.J. Mohammed, K.R. Seddon, J.A. Zora, Upon the structure of room temperature halogenoaluminate ionic liquids, J. Chem. Soc., Chem. Commun., (1986) 1753-1754.

[98] A.G. Avent, P.A. Chaloner, M.P. Day, K.R. Seddon, T. Welton, Evidence for hydrogen bonding in solutions of 1-ethyl-3-methylimidazolium halides, and its implications for room-temperature halogenoaluminate(III) ionic liquids, J. Chem. Soc., Dalton Trans., (1994) 3405-3413.

[99] J.D. Holbrey, K.R. Seddon, The phase behaviour of 1-alkyl-3-methylimidazolium tetrafluoroborates; ionic liquids and ionic liquid crystals, J. Chem. Soc., Dalton Trans., (1999) 2133-2140.

[100] G.-P. Wu, S.-H. Wei, X.-B. Lu, W.-M. Ren, D.J. Darensbourg, Highly Selective Synthesis of CO_2 Copolymer from Styrene Oxide, Macromolecules, 43 (2010) 9202-9204.

[101] G.-P. Wu, S.-H. Wei, W.-M. Ren, X.-B. Lu, B. Li, Y.-P. Zu, D.J. Darensbourg, Alternating copolymerization of CO_2 and styrene oxide with Co(III)-based catalyst systems: differences between styrene oxide and propylene oxide, Energy Environ. Sci., 4 (2011) 5084-5092.

[102] T. Ema, Y. Miyazaki, S. Koyama, Y. Yano, T. Sakai, A bifunctional catalyst for carbon dioxide fixation: cooperative double activation of epoxides for the synthesis of cyclic carbonates, Chem. Commun., 48 (2012) 4489-4491.

[103] T. Ema, Y. Miyazaki, J. Shimonishi, C. Maeda, J.-y. Hasegawa, Bifunctional Porphyrin Catalysts for the Synthesis of Cyclic Carbonates from Epoxides and CO_2: Structural Optimization and Mechanistic Study, J. Am. Chem. Soc., 136 (2014) 15270-15279.

[104] F. Castro-Gómez, G. Salassa, A.W. Kleij, C. Bo, A DFT Study on the Mechanism of the Cycloaddition Reaction of CO_2 to Epoxides Catalyzed by Zn(Salphen) Complexes, Chem. Eur. J., 19 (2013) 6289-6298.

[105] M.B. Smith, March's Advanced Organic Chemistry: Reactions, Mechanisms, and Structure, 7th Edition ed., John Wiley & Sons 2013.

[106] M. North, R. Pasquale, Mechanism of Cyclic Carbonate Synthesis from Epoxides and CO_2, Angew. Chem. Int. Ed., 48 (2009) 2946-2948.

[107] J.-Q. Wang, K. Dong, W.-G. Cheng, J. Sun, S.-J. Zhang, Insights into quaternary ammonium salts-catalyzed fixation carbon dioxide with epoxides, Catal. Sci. Technol., 2 (2012) 1480-1484.

[108] S. Foltran, R. Mereau, T. Tassaing, Theoretical study on the chemical fixation of carbon dioxide with propylene oxide catalyzed by ammonium and guanidinium salts, Catal. Sci. Technol., 4 (2014) 1585-1597.

[109] L. Wang, X. Jin, P. Li, J. Zhang, H. He, S. Zhang, Hydroxyl-Functionalized Ionic Liquid Promoted CO_2 Fixation According to Electrostatic Attraction and Hydrogen Bonding Interaction, Ind. Eng. Chem. Res., 53 (2014) 8426-8435.

[110] C.J. Whiteoak, A. Nova, F. Maseras, A.W. Kleij, Merging Sustainability with Organocatalysis in the Formation of Organic Carbonates by Using CO_2 as a Feedstock, ChemSusChem, 5 (2012) 2032-2038.

[111] F. Chen, X. Li, B. Wang, T. Xu, S.L. Chen, P. Liu, C. Hu, Mechanism of the cycloaddition of carbon dioxide and epoxides catalyzed by cobalt-substituted 12-tungstenphosphate, Chem. Eur. J. , 18 (2012) 9870-9876.

[112] H.-H. Limbach, J. Miguel Lopez, A. Kohen, Arrhenius curves of hydrogen transfers: tunnel effects, isotope effects and effects of pre-equilibria, Phil. Trans. Royal Soc. B, 361 (2006) 1399-1415.

[113] J.W. Comerford, I.D.V. Ingram, M. North, X. Wu, Sustainable metal-based catalysts for the synthesis of cyclic carbonates containing five-membered rings, Green Chem., 17 (2015) 1966-1987.

[114] A.-L. Girard, N. Simon, M. Zanatta, S. Marmitt, P. Gonçalves, J. Dupont, Insights on recyclable catalytic system composed of task-specific ionic liquids for the chemical fixation of carbon dioxide, Green Chem., 16 (2014) 2815-2825.

[115] S. Marmitt, P.F.B. Gonçalves, A DFT study on the insertion of CO_2 into styrene oxide catalyzed by 1-butyl-3-methyl-Imidazolium bromide ionic liquid, J. Comput. Chem., 36 (2015) 1322-1333.

[116] M.B. Smith, J. March, March's Advanced Organic Chemistry: Reactions, Mechanisms, and Structure, Wiley Hoboken (New Jersey, USA), 2007.